



HAL
open science

Drosophila p53 integrates the antagonism between autophagy and apoptosis in response to stress

Marion Robin, Abdul Raouf Issa, Cristiana Santos, Francesco Napoletano, Céline Petitgas, Gilles Chatelain, Mathilde Ruby, Ludivine Walter, Serge Birman, Pedro M Domingos, et al.

► **To cite this version:**

Marion Robin, Abdul Raouf Issa, Cristiana Santos, Francesco Napoletano, Céline Petitgas, et al.. Drosophila p53 integrates the antagonism between autophagy and apoptosis in response to stress. *Autophagy*, 2019, 15 (5), pp.771-784. 10.1080/15548627.2018.1558001 . hal-02396126

HAL Id: hal-02396126




<https://hal.science/hal-02396126v1>

Submitted on 5 Dec 2019

HAL is a multi-disciplinary open access archive for the deposit and dissemination of scientific research documents, whether they are published or not. The documents may come from teaching and research institutions in France or abroad, or from public or private research centers.

L'archive ouverte pluridisciplinaire **HAL**, est destinée au dépôt et à la diffusion de documents scientifiques de niveau recherche, publiés ou non, émanant des établissements d'enseignement et de recherche français ou étrangers, des laboratoires publics ou privés.

Drosophila p53 integrates the antagonism between autophagy and apoptosis in response to stress

Marion Robin^a, Abdul Raouf Issa^{b,e}, Cristiana C. Santos^c, Francesco Napoletano^{a,e}, Céline Petitgas^b, Gilles Chatelain^a, Mathilde Ruby^a, Ludivine Walter ^a, Serge Birman ^b, Pedro M. Domingos^c, Brian R. Calvi^d, and Bertrand Mollereau ^a

^aUniversité de Lyon, ENSL, UCBL, CNRS, LBMC, UMS 3444 Biosciences Lyon Gerland, Lyon, France; ^bGenes Circuits Rhythms and Neuropathology, Brain Plasticity Unit, CNRS, ESPCI Paris, Labex Memolife, PSL Research University, Paris, France; ^cInstituto de Tecnologia Química e Biológica, Universidade Nova de Lisboa, Oeiras, Portugal; ^dDepartment of Biology, Indiana University, Bloomington, IN, USA; ^eDepartment of Life Sciences, University of Trieste c/o CIB National Laboratory, Area Science Park, Trieste, Italy

ABSTRACT

The tumor suppressor TP53/p53 is a known regulator of apoptosis and macroautophagy/autophagy. However, the molecular mechanism by which TP53 regulates 2 apparently incompatible processes remains unknown. We found that *Drosophila* lacking p53 displayed impaired autophagic flux, higher caspase activation and mortality in response to oxidative stress compared with wild-type flies. Moreover, autophagy and apoptosis were differentially regulated by the p53 (p53B) and ΔNp53 (p53A) isoforms: while the former induced autophagy in differentiated neurons, which protected against cell death, the latter inhibited autophagy by activating the caspases Dronc, Drice, and Dcp-1. Our results demonstrate that the differential use of p53 isoforms combined with the antagonism between apoptosis and autophagy ensures the generation of an appropriate p53 biological response to stress.

ARTICLE HISTORY

Received 17 October 2016
Revised 7 December 2018
Accepted 7 December 2018

KEYWORDS

Apoptosis; caspase;
Drosophila melanogaster;
macroautophagy;
neurodegenerative disease;
oxidative stress; p53;
Parkinson disease;
photoreceptor

Introduction

Since its discovery more than 30 years ago, TP53/TRP53/p53 has been recognized to be a major tumor suppressor protein that functions principally through effects on apoptosis, cell cycle arrest, and DNA repair [1,2]. Although non-canonical functions of TP53/TRP53/p53 in cell metabolism, autophagy, necrosis, and proliferation have recently been studied in detail, their roles in tumorigenesis have yet to be determined [3–5].

Autophagy is an intracellular multistep process responsible for the degradation and recycling of cytoplasmic contents by lysosomal proteases [6]. The first step in autophagy is formation of a double-membrane structure that engulfs cytoplasmic components, such as protein aggregates and damaged organelles, and matures to form a vesicle known as an autophagosome. In turn, the autophagosome fuses with a lysosome to form an autolysosome. This process culminates in degradation of the vesicle contents, a phenomenon known as autophagic flux. For proper functioning, autophagy requires both vesicle formation and autophagic flux [7]. Autophagy is a prosurvival mechanism required for the removal of damaged organelles or misfolded proteins and the impairment of autophagic flux is commonly observed in neurodegenerative diseases [8].

One of the key unanswered questions in TP53/TRP53/p53 biology concerns the mechanisms by which TP53/TRP53/p53 induces different responses following exposure to stress. The

answer may lie in the multiple transcriptional targets and cofactors differentially activated by TP53/TRP53/p53, depending on the cellular and environmental context. It has been suggested that TP53/TRP53/p53 target genes induce reactive oxygen species (ROS) detoxification and DNA repair in low-stress conditions and induce senescence and apoptosis in high-stress conditions [1]. The study of TP53/TRP53/p53 isoforms provides some interesting clues on how TP53/TRP53/p53 achieves specific cellular responses [9]. In humans, the TP53/p53 protein is expressed as 12 isoforms that are generated by 2 internal promoters and alternative splicing and codon initiation sites [10,11]. In *Drosophila*, genome annotations have predicted the existence of 3 *Drosophila* p53 protein isoforms (FlyBase FBgn0039044) (Figure S1A) [12]. The best-studied isoform is ΔNp53 (p53A), which has a 110-amino acid deletion in its transactivation domain and is structurally analogous to the N-terminally truncated human TP53/p53 isoforms [13–15]. The p53 (p53B) isoform refers to the full-length p53 protein that has an intact transactivation domain and is structurally analogous to the human full-length TP53/p53 [9,16,17]. The third, most recent discovered isoform, p53E, is a 334-amino acid protein with a unique 10-amino acid transactivation domain which presumably acts as a dominant negative [18].

An alternative possibility to explain TP53/TRP53/p53 pleiotropic functions is that TP53/TRP53/p53 may induce multiple pathways simultaneously. For example, the TP53/

TRP53/p53 target DRAM is involved in the regulation of both autophagy and apoptosis [19,20]. However, the molecular mechanisms enabling a single *TP53/Trp53/p53* gene to regulate 2 apparently incompatible processes – autophagy (pro-survival) and apoptosis (pro-death) – in the same cellular context remain unclear. Presumably, there must be antagonism between the pathways to ensure that TP53/TRP53/p53 does not induce conflicting signals, but instead favors the most response appropriate for the particular cell type and stress intensity. Simple organisms, such as *Drosophila*, have proved useful for studying the primordial functions of TP53/TRP53/p53, such as induction of apoptosis in response to irradiation [13–15,21], and for examining a wide range of less-studied functions, including differentiation, growth, neuroprotection, proliferation, and meiotic recombination [5,17,22–27].

In this study, we investigated the relationship between p53-regulated autophagy and apoptosis in *Drosophila*. We found that p53 protected the organism from ROS. Interestingly, *Drosophila* lacking *p53* displayed impaired autophagic flux, higher caspase activation and mortality levels upon paraquat treatment. We also found that autophagy and apoptosis were differentially regulated by the p53 isoforms. Whereas the p53 (p53B) isoform induced protective autophagy in adult neurons, the $\Delta Np53$ (p53A) isoform inhibited autophagy by activating the caspases Dronc, Drice, and Dcp-1. These findings uncover a novel layer of p53-mediated regulation of life and death via differential activation of autophagy and apoptosis.

Results

Redundant roles of p53 isoforms in the resistance to ROS

To investigate the importance of p53 in the stress response at the whole-organism level, we first exposed wild-type (WT, *w¹¹¹⁸*) and *p53^{null}* (*p53^{5A-1-4}*, null mutant for all the isoforms) flies to ROS by feeding them with 20 mM paraquat (PQ)-containing medium. PQ is a free radical-inducing agent that has been widely used to induce ROS in cells and organisms [28–30]. We found that *p53^{null}* flies were more sensitive than control flies to PQ-induced ROS, with the median time to 50% lethality being reached at ~20 h compared with ~48 to 72 h (Figure 1(a)). Furthermore, *p53^{null}* flies rescued by a genomic construct that encompasses the *p53* locus (*p53Bac*, *p53^{5A1-4}*) showed a PQ sensitivity similar to that of WT flies (Figure 1(a)), which confirms that PQ-sensitivity maps to the *p53* locus. To study the physiological function of the $\Delta Np53$ (p53A) and p53 (p53B) isoforms under conditions of oxidative stress, we first examined the levels of $\Delta Np53$ (p53A) and *p53* (p53B) transcripts in animals exposed to PQ (Figure S1B). We observed that while $\Delta Np53$ (p53A) transcripts were unchanged by PQ, *p53* (p53B) transcripts were increased 3-fold, suggesting that p53 (p53B) may play an important role in the PQ response. Next, we examined transcript levels in 2 characterized p53 isoform mutants [18]. *Ch-p53B STOP*; *p53^{5A-1-4}* (here named *Ch-p53B STOP*) which is mutant for p53 (p53B) but encodes the

$\Delta Np53$ (p53A) isoform and *GFP-p53A STOP*; *p53^{5A-1-4}* (here named *GFP-p53A STOP*) which is mutant for $\Delta Np53$ (p53A) but encodes p53 (p53B) isoform. The p53E isoform lacks most of the transactivation domain, having a dominant negative effect; therefore, we excluded it from our study. As predicted, *Ch-p53B STOP* flies do not express *p53* (p53B) but had normal levels of $\Delta Np53$ (p53A) transcripts (Figure S1C), which is consistent with previous data [18]. To our surprise, the *GFP-p53A STOP* mutant lacked both *p53* (p53B) and $\Delta Np53$ (p53A) transcripts, which is not observed in the earlier study for technical reasons [18]. We thus excluded the *GFP-p53A STOP* mutant from further analyses and focused on the *p53* (p53B) mutant (*Ch-p53B STOP*) in which $\Delta Np53$ (p53A) is functional. We compared PQ toxicity in *Ch-p53B STOP*, *p53^{null}*, and WT flies and observed that while *p53^{null}* mutant showed an increase sensitivity to PQ there was no difference in the survival of *Ch-p53B STOP* and WT flies (Figure S1D). To further assess the role of $\Delta Np53$ (p53A) in the resistance of flies to PQ treatment, we used CRISPR/Cas9 method to generate $\Delta Np53$ (p53A) mutant flies, named the *p53^{A2.3}* mutant line, carrying a small deletion removing the coding and splice donor of the $\Delta Np53$ (p53A) unique exon, which impairs the $\Delta Np53$ (p53A) isoform (Figure S2). We thus compared PQ toxicity in *p53^{A2.3}* mutant, *p53^{null}*, and WT flies and observed no difference in the survival of *p53^{A2.3}* and WT flies (Figure S2C). Together, these results show that the inactivation of both $\Delta Np53$ (p53A) and p53 (p53B) isoforms in *p53^{null}* mutant flies, but not the individual loss of $\Delta Np53$ (p53A) (*p53^{A2.3}*) or *p53* (p53B) (*Ch-p53B STOP*, *p53^{-/-}*), confers an increased sensitivity to PQ treatment. This indicates that $\Delta Np53$ (p53A) and p53 (p53B) isoforms play redundant functions in the resistance to PQ.

p53^{null} mutant flies have a defective autophagic response in response to paraquat

The sensitivity of *p53^{null}* flies to PQ is similar to that of autophagy-defective mutant flies, which are extremely sensitive to ROS (Figure 1(b)) [31,32]. Together with the fact that TP53/TRP53/p53 is a known regulator of autophagy [20,33], it raises the possibility that autophagy may be defective in *p53^{null}* flies. To investigate this, we examined the expression of ref(2)P/SQSTM1/p62, a multifunctional scaffold protein that is degraded during autophagy and accumulates in the cytoplasm of autophagy-defective *atg8a* mutants [34]. We found that ref(2)P levels were higher in *p53^{null}* flies than control flies exposed to PQ (Figure 1(c) and S3A). ref(2)P accumulation was also observed in *atg8a^{-/-}* flies, as previously described [34]. The accumulation of ref(2)P could be due a reduced activation of autophagy in flies lacking p53. However, we did not observe a p53-dependent induction of the Atg8a-II:Atg8a-I ratio in WT flies after PQ treatment. In contrast, the Atg8a-II:Atg8a-I ratio was lower in *p53^{null}* compared to control flies exposed to PQ, indicating that p53 was not activating autophagy but rather that basal autophagy levels were reduced in the *p53* mutant (Figure 1(d)). Thus, *p53^{null}* flies exhibit an increased sensitivity to ROS, which is associated with

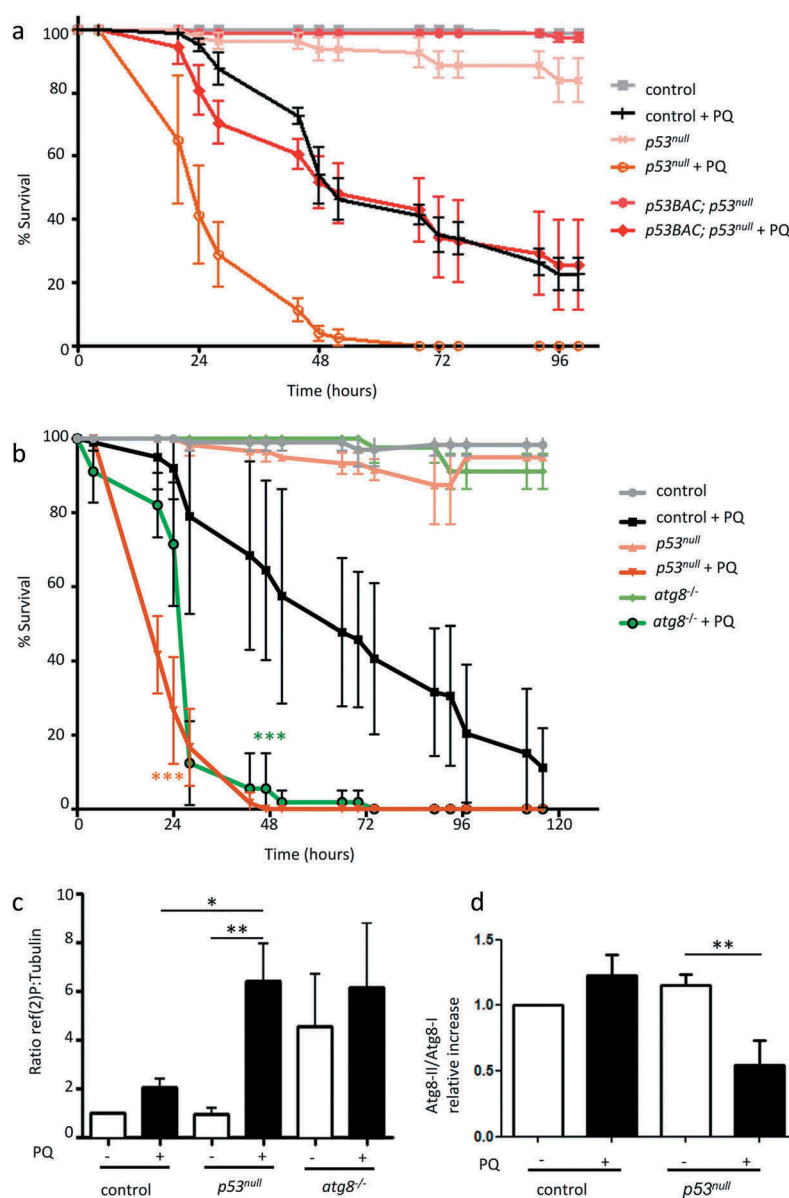


Figure 1. p53- and autophagy-mutant flies show increased sensitivity to paraquat. (a and b) Survival curves of wild-type and mutant *Drosophila* fed with normal or 20 mM paraquat (PQ)-containing media (A, $n = 4$ and B, $n = 5$). 1) Control, *w1118* flies, 2) *p53^{null}* (*p53^{5A1-4}* mutants), 3) *p53BAC*, *p53^{null}* flies carrying a wild-type *p53* genomic rescue BAC clone on the second chromosome and 4) *atg8^{-/-}*, (*atg8^{KG07569}* mutants). (c) Densitometric quantification of endogenous ref(2)P levels in whole flies fed with normal or PQ-containing media. Data are the mean \pm SEM of 5 independent blots and are presented as the ratio of ref(2)P:tubulin in experimental animals relative to the ratio in control non-treated flies. * $P < 0.05$, ** $P < 0.01$ by one-way ANOVA followed by the Bonferroni post hoc test. (d) Quantification of Atg8-II:Atg8-I from western blots of control and *p53^{null}* flies treated or non-treated with PQ. Data are the mean \pm SEM of $n = 3$ blots and are presented as expression levels relative to that in non-treated control flies.

a reduced basal autophagy and an increased ref(2)P levels, suggesting an impairment in the autophagic flux.

Next, we asked whether the increased sensitivity to PQ is associated with increased caspase activation in *p53^{null}* flies. Since one of the primary targets of PQ toxicity is the nervous system [35], we investigated whether loss of p53 resulted in caspase activation in whole flies or fly brains after exposure to PQ. Western blot analysis and immunostaining using specific antibodies [17,36] revealed a strong increase in the cleaved form of Dcp-1 and immunoreactivity detected by an anti-cleaved human CASP3 antibody in *p53^{null}* and *atg8a^{-/-}* mutant flies following exposure to PQ in 4-day-old flies (Figure 2(a-h) and S3B). The anti-cleaved human CASP3 antibody, which

recognizes the cleaved effector caspases, Drice and Dcp-1 reflects Dronc activity [37]. This increase was evident by western blotting of whole flies (Figure 2(a,b)), fly heads (Figure S3B) and by immunostaining of adult brains (Figure 2(c-h)). In the brain, cells positive for immunoreactivity detected with an anti-cleaved, human CASP3 antibody, could be detected in the whole brain cortex, particularly in the dorsolateral and dorsomedial protocerebrum, after PQ treatment (Figure 2(c-h)). Although caspase activation was not detected in WT whole flies by western blotting, it could be observed in dissected brains by immunostaining (Figures 2(f,h)). Collectively, these results suggest that the elevated sensitivity of *p53^{null}* mutant flies to oxidative stress injury leads to an increase in apoptosis.

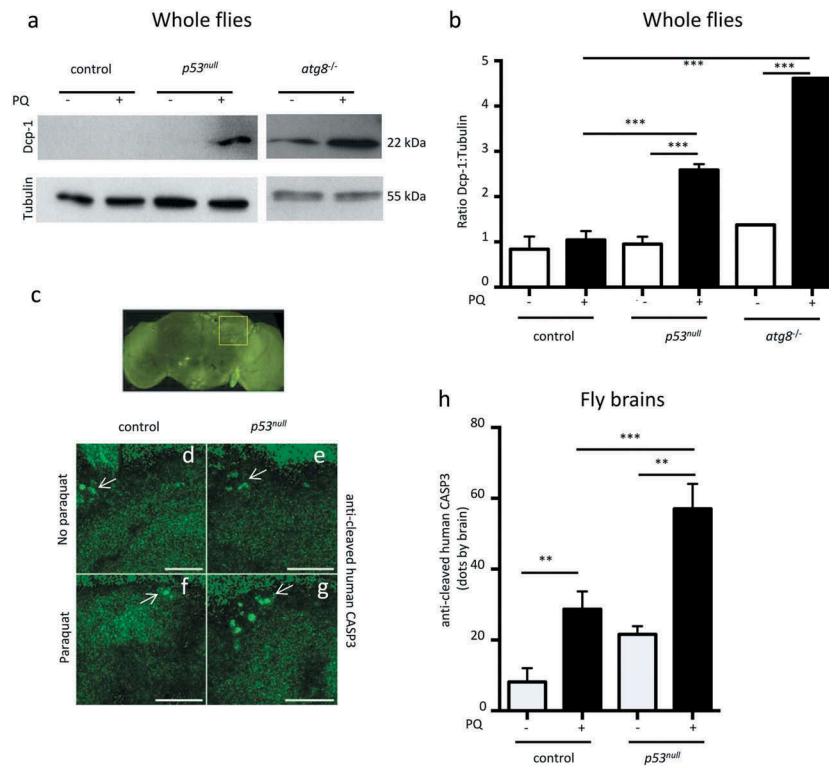


Figure 2. *p53*- and autophagy-defective flies show increased caspase activation after paraquat treatment. (a and b) Representative western blot and densitometric quantification of endogenous cleaved Dcp-1 in whole flies. Data are the mean \pm SEM of 3 independent blots and are expressed as the ratio of cleaved Dcp-1:tubulin. $***P < 0.001$ by one-way ANOVA followed by the Bonferroni post hoc test. (c) Dorsomedial protocerebrum area of the fly brain selected for quantification of immunoreactivity to an anti-cleaved human CASP3 antibody (yellow box). (d–g) Representative images of the above-mentioned cleaved human CASP3 immunostaining in the dorsomedial protocerebrum of untreated control (d) and *p53^{-/-}* (e) flies or PQ-treated control (f) and *p53^{-/-}* (g) flies. Scale bars: 25 μ m. White arrows show cells positively stained for cleaved human CASP3. (h) Quantification of staining with immunoreactivity against cleaved human Caspase 3 counted in the dorsomedial protocerebrum. $**P < 0.01$, $***P < 0.001$ by one-way ANOVA followed by the Bonferroni post hoc test.

Δ Np53 (p53A)-dependent caspase activation inhibits autophagic flux in the Drosophila eye

The observation that *p53^{null}* flies display defective autophagic flux and increased apoptosis following exposure to PQ prompted us to study the regulation of autophagy and apoptosis by p53 at the cell and tissue level. We used *Drosophila* photoreceptor cell (PR) neurons as a model to overexpress Δ Np53 (p53A) and p53 (p53B) in a WT background [38]. Because the isoforms differentially regulate caspase activation, this system allowed us to directly examine the influence of p53 isoforms on caspase activation and the autophagic response in adult PRs (Figure S4) [39]. When the isoforms were ectopically expressed in adult PRs, we found that Δ Np53 (p53A), similar to the apoptosis protein Rpr (Reaper), induced robust activation of Dcp-1 and apoptosis, whereas p53 (p53B) had no detectable induction of Dcp-1 compared to control (Figure S4A to D). In agreement with the lack of activated Dcp-1 induced by p53 (p53B), the expression of the caspase inhibitor p35 only suppressed Dcp-1 staining and PR degeneration induced by Rpr and Δ Np53 (p53A) but not PR degeneration induced by p53 (p53B). (Figure S4E–I). These results indicate that Δ Np53 (p53A) induces PR apoptosis while p53 (p53B) promotes caspase-independent PR degeneration.

To assess whether the expression of p53 (p53B) and Δ Np53 (p53A) induces autophagy, we visually monitored the formation of autophagy vesicles in the PRs using a GFP-tagged form of Atg8a/LC3 (GFP-Atg8a) as a reporter. Overexpression of either p53 (p53B) or Δ Np53 (p53A) in PRs increased the number of GFP-Atg8a dots compared with cells overexpressing a control protein, indicating a greater abundance of autophagy vesicles in the cytoplasm (Figure S5A to C and S5G). The induction of autophagy by *Drosophila* p53 isoforms was also confirmed by the presence of autophagic vacuoles visualized by transmission electron microscopy (TEM) in PR expressing p53 (p53B) or Δ Np53 (p53A) (Figure S5H and S5I).

The increase in autophagic vesicles could result from activation of autophagy, leading to an increase in autophagosome formation, and/or from inhibition of autophagic flux, leading to an accumulation of unprocessed vesicles, as observed in flies overexpressing the polyglutamine protein, Gug/Atro (termed Gug/Atro75QN subsequently in the text) [40]. To distinguish between these 2 possibilities, we assessed autophagic flux by expressing GFP-ref(2)P and mCherry-GFP-Atg8a reporters in PRs (Figures 3 and 4). GFP-ref(2)P offers an advantage over immunostaining of endogenous ref(2)P because its accumulation is independent of *ref(2)P* promoter

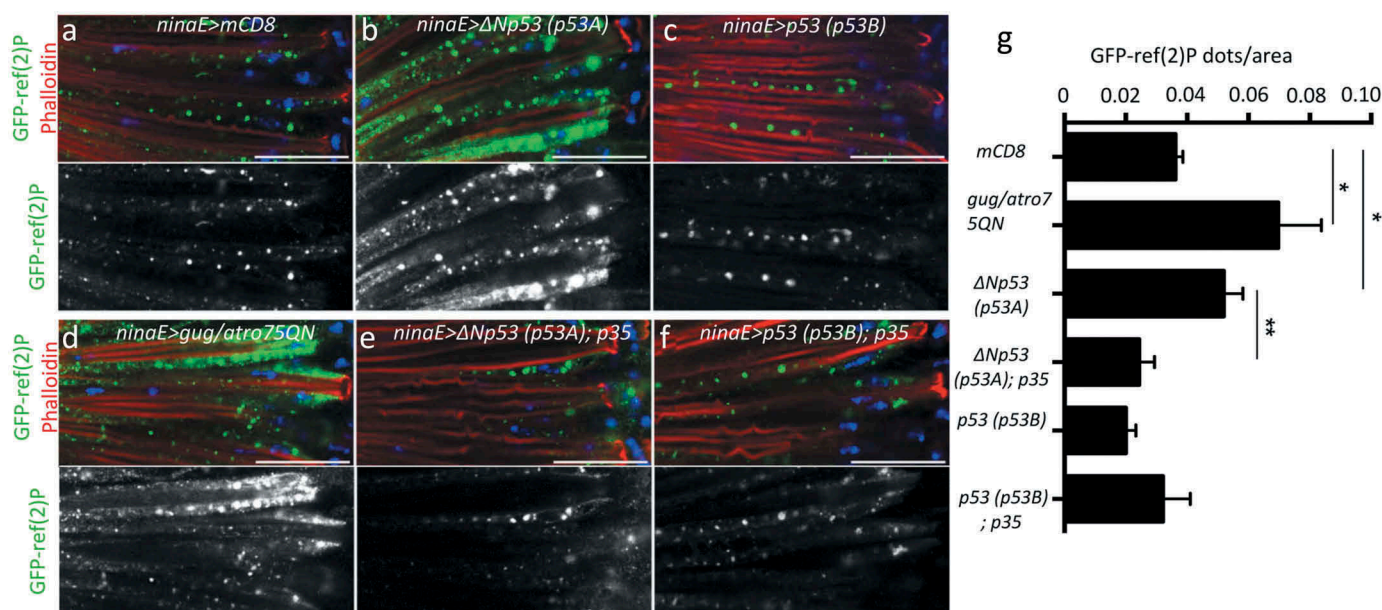


Figure 3. Differential ref(2)P processing in photoreceptors expressing p53 (p53B) or Δ Np53 (p53A). (a–f) Representative fluorescence microscopy images of the retinas of adult flies expressing autophagic flux reporter *GFP-ref(2)P* in photoreceptors (PRs). The nuclei were stained with DAPI (blue). Flies also overexpressed *mCD8-RFP* (control protein), Δ Np53 (p53A), p53 (p53B), *gug/atro75QN*, Δ Np53 (p53A) and p35, or p53 (p53B) and p35 in PRs under the control of *ninaE/rh1-GAL4*. Actin was visualized by staining with phalloidin (red). Scale bars: 20 μ m. (g) Quantification of GFP-ref(2)P dots per retina in the strains represented in (a–f) using the Find Maxima function of ImageJ software. Data are the mean \pm SEM of $n = 8$ to 15 retinas. * $P < 0.05$, ** $P < 0.01$ by the Student t test.

regulation by ROS [41] and it therefore unambiguously reflects autophagy impairment. As expected, PRs overexpressing *Gug/Atro75QN* accumulated more GFP-ref(2)P than did control PRs, indicating that autophagic flux was blocked (Figure 3(a,d,g)). We observed a clear difference in autophagic flux between cells overexpressing p53 (p53B) and Δ Np53 (p53A). GFP-ref(2)P levels were unchanged by p53 (p53B) overexpression compared to control (Figure 3(a,c,g)), indicating normal autophagic flux, whereas overexpression of Δ Np53 (p53A) led to an accumulation of GFP-ref(2)P similar to what was observed in PRs overexpressing *Gug/Atro75QN* (Figure 3(a,b,d,g)). The same effects of p53 (p53B) and Δ Np53 (p53A) overexpression were observed when autophagic flux was measured using the mCherry-GFP-Atg8a reporter (Figure 4). In PRs expressing this reporter, autophagosomes appear yellow since they emit both GFP and mCherry fluorescence, while autolysosomes emit only mCherry fluorescence due to quenching of eGFP in the acidic environment [7,42,43]. We observed more mCherry than GFP fluorescence in PRs expressing p53 (p53B), indicating the presence of autolysosomes and an intact autophagic flux (Figure 4(a,c)). In contrast, mCherry was more colocalized with GFP in PR cells overexpressing Δ Np53 (p53A) compared to p53 (p53B) (Figure 4(a–c)). The perdurance of both GFP and Cherry staining in autophagic vacuoles, reflects a relative paucity of autolysosomes and an inhibition of autophagic flux by Δ Np53 (p53A), perhaps due to a failure of autophagosomes and lysosomes to fuse or a lack of degradative enzymes in autolysosomes (Figures 4(b,c,g)). Taken together, these results demonstrate that Δ Np53 (p53A), but not p53 (p53B), inhibits the autophagic flux in PRs.

We hypothesized that the differential effects of Δ Np53 (p53A) and p53 (p53B) on autophagic flux may be due to

differences in caspase activation by the 2 isoforms (Figure S4C and S4D). To test this hypothesis, we compared levels of GFP-Atg8a, GFP-ref(2)P, and mCherry-GFP-Atg8a in cells concomitantly expressing either p53 (p53B) or Δ Np53 (p53A) and the effector caspase inhibitor p35. We found that concomitant expression of Δ Np53 (p53A) and p35 resulted in lower levels of GFP-Atg8a (Figure S5A, S5B, S5E and S5G) and of GFP-ref(2)P (Figure 3(a,b,e,g)) compared to PRs overexpressing Δ Np53 (p53A) alone. This indicates that the inhibition of caspases by p35 restores the defective autophagic flux in PR expressing Δ Np53 (p53A). Similarly, concomitant expression of Δ Np53 (p53A) and p35 reduced the levels of GFP and the colocalization of GFP and Cherry, compared to Δ Np53 (p53A)-overexpressing PRs carrying mCherry-GFP-Atg8a (Figure 4(a,b,d,e,g)). In contrast, p35 had no effect on GFP-Atg8a, GFP-ref(2)P and mCherry-GFP-Atg8a levels when coexpressed with p53 (p53B) (Figures S5F, S5G, 3F, 3G, 4F and 4G). This was expected because p53 (p53B) expression does not induce caspase activation (Figure S4D). Expression of p35 alone induced a reduction of basal GFP-Atg8a and GFP-ref(2)P levels in control PRs suggesting that low level of caspase activation, which is not detected with the antibody against cleaved Dcp-1, inhibits autophagic flux in wild type retina (Figure S5J and S5K). Collectively, our results indicate that Δ Np53 (p53A)-dependent activation of caspases inhibits autophagic flux in adult *Drosophila* PRs.

***Dronc*, *Dcp-1*, and *Drice* are required for inhibition of autophagic flux by Δ Np53 (p53A)**

Having shown that caspase activation induced by Δ Np53 (p53A) impairs autophagic flux, we next asked whether the

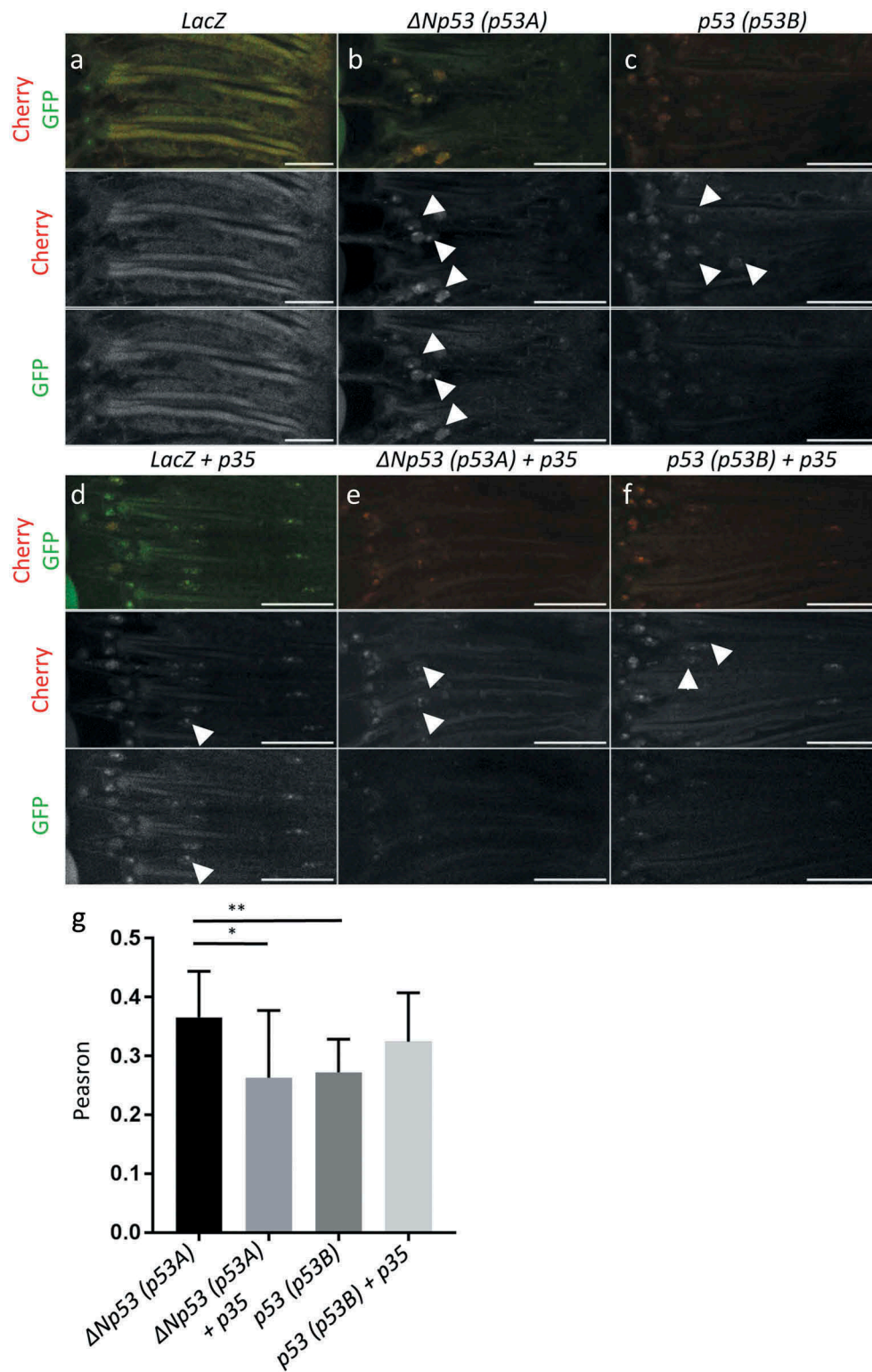
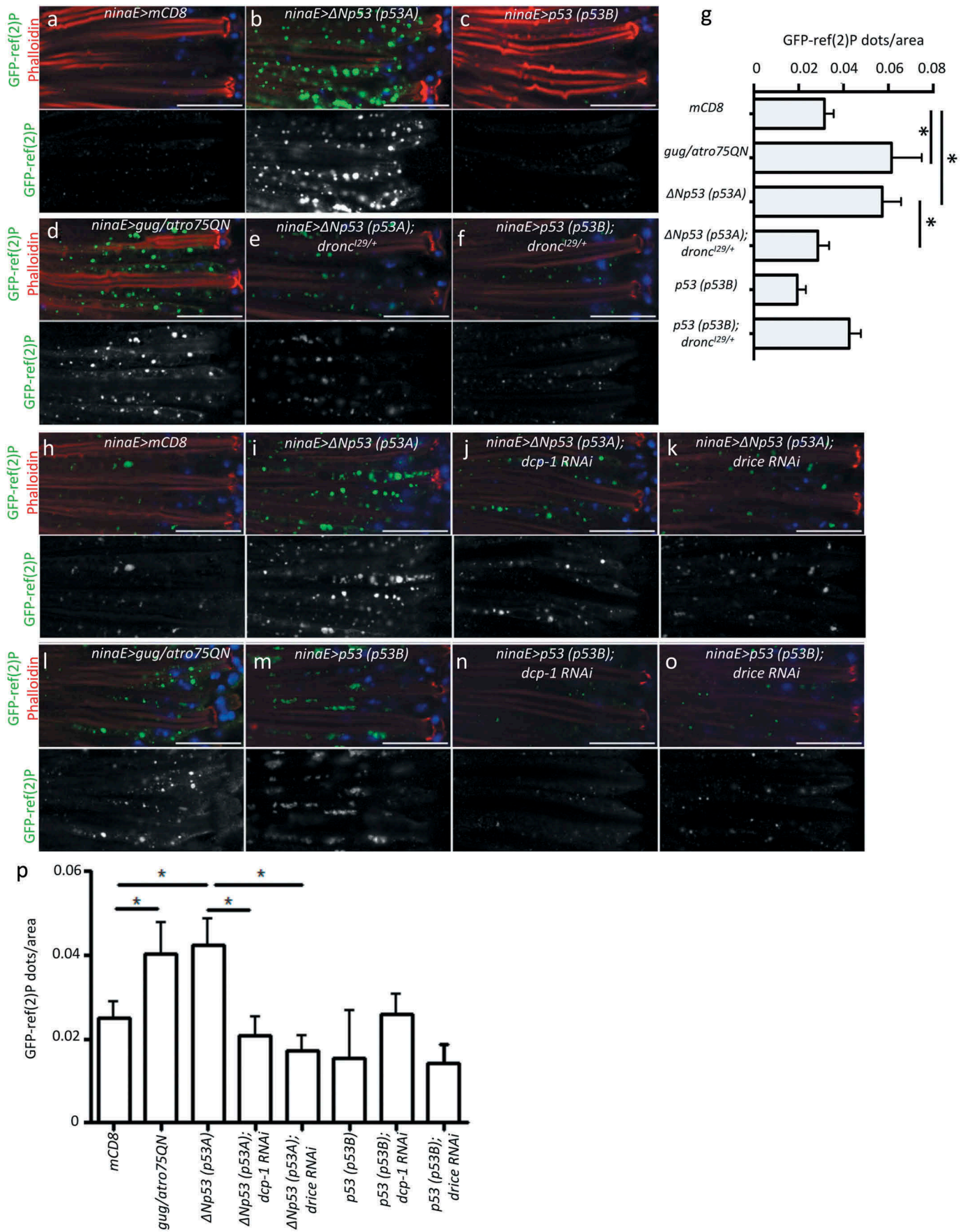


Figure 4. Differential processing of mCherry-GFP-Atg8 in *p53* (*p53B*)- and $\Delta Np53$ (*p53A*)-expressing flies. (a–f). Representative fluorescence microscopy images of the retina of adult flies overexpressing the autophagy reporter mCherry-GFP-Atg8 plus *LacZ* (control) \pm *p35*, $\Delta Np53$ (*p53A*) \pm *p35*, and *p53* (*p53B*) \pm *p35* driven by *ninaE/rh1-GAL4*. mCherry in red and GFP is green. Staining from $n = 2$ to 10 retinas. Arrowheads show high levels of GFP-positive dots. Scale bars: 10 μ m. (g) Quantification of colocalization of cherry and GFP staining by the Pearson coefficient from A to F, $n = 15$ –26 retinas * $P < 0.05$, ** $P < 0.01$ by one way Anova followed by the Tukey multiple comparison test.

initiator caspase Dronc and the effector caspases Dcp-1 and Drice contribute to this effect. We found that heterozygous *dronc* mutations decreased the GFP-ref(2)P accumulation

induced by $\Delta Np53$ (*p53A*) to basal levels, similar to those seen in WT retinas (Figure 5(a,b,e,g)). Moreover, RNAi-mediated knockdown of *dcp-1* abolished cleaved Dcp-1



staining in PRs expressing Δ Np53 (p53A) (Figure S6C and S6D) and decreased GFP-ref(2)P to the level seen in control PRs (Figure 5(h,j,p)). RNAi-mediated *drice* knockdown also led to a decrease in GFP-ref(2)P levels in PRs expressing Δ Np53 (p53A) (Figure 5(h,k,p)). As a control, knockdown of *dcp-1* or *drice* had no significant effects on GFP-ref(2)P levels in PRs expressing p53 (p53B) or in control PRs (Figure 5(m,n,o,p) and S6E). Thus, activation of Dronc, Dcp-1, and Drice is required for Δ Np53 (p53A) to inhibit processing of autophagy vesicles.

Induction of autophagy protects PRs from p53 (p53B)-induced death

We showed that the overexpression of p53 (p53B) does not induce caspase activation but instead induces progressive caspase-independent PR death and concomitant activation of functional autophagy. By contrast, Δ Np53 (p53A) overexpression induces caspase activation, subsequent inhibition of autophagic flux and PR death. We therefore investigated the role of p53 (p53B)-dependent autophagy in PR survival. We overexpressed p53 (p53B) or Δ Np53 (p53A) in retinas carrying *atg1* mutant clones by using the Tomato-GFP-FLP-FRT method, and evaluated PR survival in young flies at a time before extensive cell death has occurred [44,45]. Expression of Δ Np53 (p53A) resulted in similar levels of cell death in WT (labeled with tomato and GFP) and *atg1* mutant (labeled GFP and the absence of tomato) PRs (Figure 6(c,e)). This finding was expected because autophagy is impaired by expression of Δ Np53 (p53A) in WT retinas (Figures 3 and 4). By contrast, the rate of p53 (p53B)-induced PR death was higher in *atg1* mutant cells compared to the surrounding area of WT PRs (Figure 6(d,e)). Overall, these results indicate that p53 (p53B) induces functional autophagy that protects PRs from p53 (p53B)-induced neurodegeneration.

Discussion

To gain a better understanding on how p53 can orchestrate cell survival and cell death through various and antagonistic pathways, we have studied the consequences of p53 neuronal gain of function and of paraquat-induced oxidative stress in presence or absence of p53. Neuronal expressions of Δ Np53 (p53A) or p53 (p53B), 2 protein isoforms of *Drosophila* p53, are both efficient inducers of autophagy but each isoform induces a differential regulation of autophagy (Figure 7): p53 (p53B) induces a functional autophagy, while Δ Np53 (p53A) induces a defective autophagic flux. Indeed, the net contribution of Δ Np53 (p53A) on autophagy is reduced compared to

that of p53 (p53B) by the concomitant activation of caspases, which inhibits the autophagic flux. These results also indicate that there must be antagonism between apoptosis and autophagy to ensure that p53 does not induce conflicting signals, and instead promotes the appropriate response for the particular cell type and stress intensity. For example, we, and others, have shown that autophagy protects against neuronal death by inhibiting apoptosis [46–48]. Here, we observed the reverse effect, with caspase activation leading to the inhibition of autophagic flux. Specifically, we showed that the initiator caspase Dronc and the effector caspases Drice and Dcp-1 are required to inhibit the autophagic flux. Thus, the mutual antagonism between apoptosis and autophagy ensures that one of these responses is preferentially induced depending on the cellular context. Two studies have shown that Dcp-1 regulates autophagy in *Drosophila* [49,50]. In the first study, Kramer et al. show that Dcp-1 inhibits quality control autophagy in developing PRs [49]. In contrast to our finding that Dcp-1 inhibits autophagy by blocking autophagic flux, they show that Dcp-1 inhibits the induction of autophagy in the WT retina by cleaving Acn (Acinus). We thus favor the hypothesis that Dcp-1 has different and currently unidentified targets for regulating autophagic flux in differentiated PRs. In the second study, the Gorski group examines starvation-induced degeneration of the mid-stage egg chamber; in this case, Dcp-1 is required for cell death and autophagy [50,51]. Also in contrast to our finding that Dcp-1 inhibits autophagic flux, they show that Dcp-1 increases autophagic flux by interacting in a proteolysis-independent manner with mitochondrial adenine nucleotide translocase stress-sensitive B (SesB). Collectively, these findings and our own show that Dcp-1 can regulate the induction of autophagy and autophagic flux in multiple ways depending on the cell type and developmental stage. Thus, the outcome – cell survival or death – depends not only on the differential expression of p53 isoforms but also on their ability to activate 2 mutually antagonistic responses, autophagy or apoptosis, that are independently responsive to the prevailing conditions.

The differential regulation of apoptosis by TRP73/p73 isoforms has also been studied in mouse neuronal culture submitted to neurotoxic expression of A β protein [52]. In this model of neurodegeneration, TRP73 β promotes while Δ NTRP73 inhibits apoptosis, which is opposite to our observation that Δ Np53 promoted apoptosis while p53-induced caspase-independent cell death in flies. Furthermore, the differential expression of human TP53 isoforms Δ 133TP53 and TP53 β in astrocytes is important to confer neuroprotection in cellular models of Alzheimer disease and amyotrophic lateral sclerosis [53]. Thus, further work is needed to define the

Figure 5. Inhibition of Dronc, Drice, or Dcp-1 restores ref(2)P processing in photoreceptors expressing Δ Np53 (p53A). (a–f) Representative fluorescence microscopy images of the retinas of adult flies expressing the autophagic flux reporter GFP-ref(2)P in photoreceptors (PRs). Flies also overexpressed mCD8-RFP (control protein), Δ Np53 (p53A), p53 (p53B), *gug/atro75QN*, Δ Np53 (p53A) and *dronc*¹²⁹, or p53 (p53B) and *dronc*¹²⁹ in PRs under the control of *ninaE/rh1-GAL4*. *Dronc*¹²⁹ flies carry one *dronc*¹²⁹ mutant allele. Actin and cell nuclei were visualized by staining with phalloidin (red) and DAPI (blue), respectively. Scale bars: 20 μ m. (g) Quantification of GFP-ref(2)P dots per retina area in the strains represented in (a–f). Data are the mean \pm SEM of $n = 8$ to 17 retinas. * $P < 0.05$ by the Student t test. (h–o) Representative images of the retina of adult flies expressing the autophagic flux reporter GFP-ref(2)P in PRs. Flies also overexpressed mCD8-RFP (control), Δ Np53 (p53A), Δ Np53 (p53A) with *dcp-1RNAi*, Δ Np53 (p53A) with *drice-1RNAi*, *gug/atro75QN*, p53 (p53B), p53 (p53B) with *dcp-1RNAi*, or p53 (p53B) with *drice-1RNAi* under the control of *ninaE/rh1-GAL4*. Actin and cell nuclei were visualized by staining with phalloidin (red) or DAPI (blue), respectively. Scale bars: 20 μ m. (p) Quantification of GFP-ref(2)P dots per retina area in the strains represented in (h–o). Data are the mean \pm SEM of $n = 8$ to 15 retinas. * $P < 0.05$ by the Student t test.

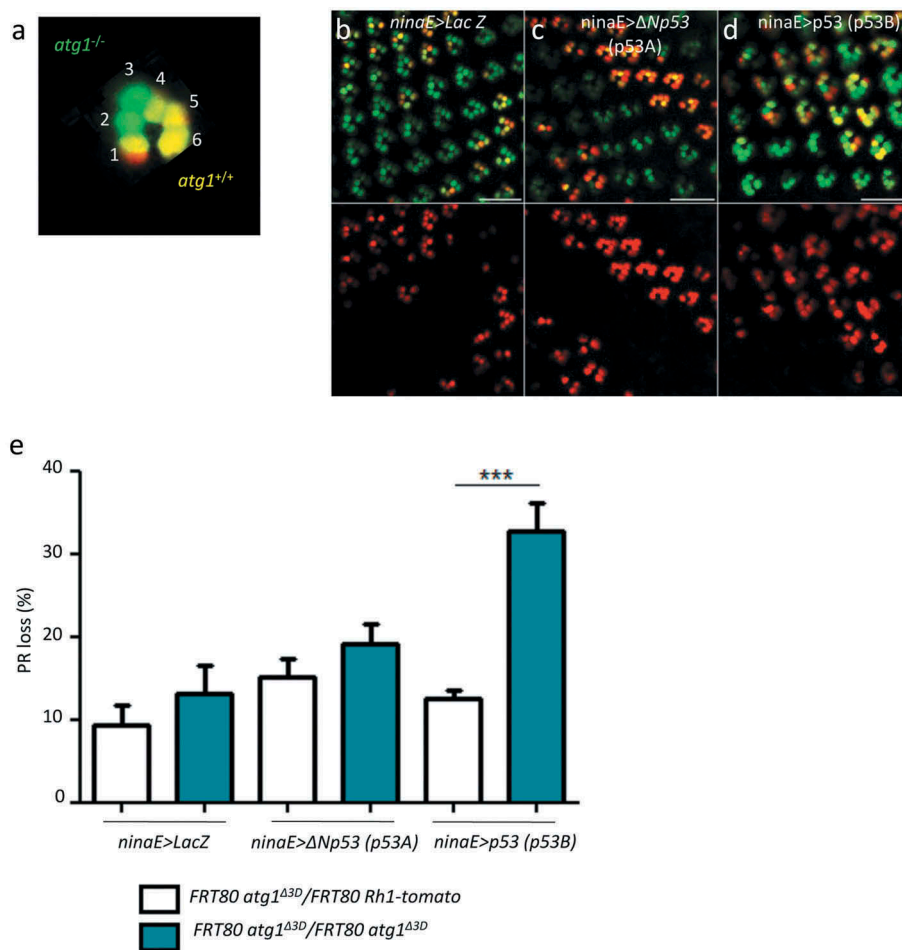


Figure 6. *atg1* mutant photoreceptors show increased sensitivity to p53 (p53B)-induced, but not Δ Np53 (p53A)-induced death. Ommatidia from flies overexpressing *LacZ* (control), Δ Np53 (p53A), or p53 (p53B) in PRs under the control of *ninaE/rh1-GAL4*. (a) Representative mosaic ommatidia with wild-type (*ey-flp*, *ninaE/rh1-GAL4*; *UAS-GFP*; *FRT80 atg1 Δ 3D/FRT80 ninaE/Rh1-tomato*) and *atg1^{-/-}* mutant (*ey-flp*, *ninaE/rh1-GAL4*; *UAS-GFP*; *FRT80 atg1 Δ 3D/FRT80 atg1 Δ 3D*) PRs, as generated for (b–d). Numbers 1 to 6 indicate the outer PRs (R1–6). Wild-type PRs carry 2 copies of Tomato in addition to GFP and thus appear yellow. Mutant clones, in green, were generated by mitotic recombination and thus carry GFP but not the Tomato reporter. (b–d) Representative retinas showing *atg1 Δ 3D* mutant clone size. Scale bars: 20 μ m. (e) Quantification of PR loss in wild-type and mutant clones from $n = 12$ to 14 retinas. Data are shown as global PR loss per fly strain. *** $P < 0.001$ by the Student t test.

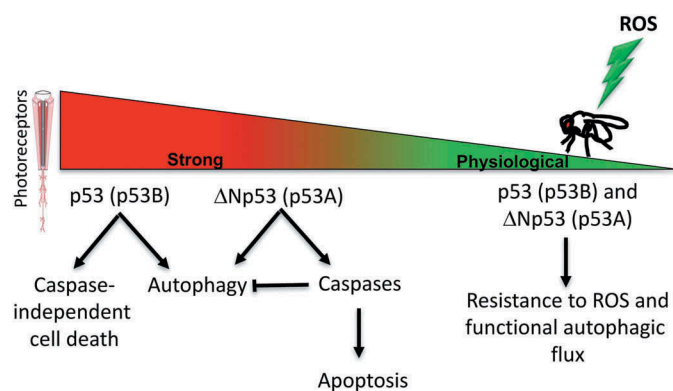


Figure 7. Life and death: levels of p53 isoforms matter. (Left) When p53 isoforms are overexpressed in photoreceptor neurons at high levels, p53 (p53B) induces autophagy and caspase-independent cell death, while Δ Np53 (p53A) induces caspase activation and inhibits autophagic flux. (Right) Physiological levels of p53 isoforms confer redundant resistance to reactive oxygen species (ROS) and a functional autophagic flux. Pink schematic labeled photoreceptors on the left represents one ommatidium containing 8 photoreceptor neurons and accessory cells.

conserved roles of TP53 and TRP73 family isoforms in neurodegeneration and protection.

This study reveals the importance of Δ Np53 (p53A) and p53 (p53B) in response to OS. It also shows that both Δ Np53 (p53A) and p53 (p53B) confer redundant resistance to OS induced by PQ. This indicates that physiological levels of both p53 isoforms are required for the organismal survival. A physiological role of both Δ Np53 (p53A) and p53 (p53B) isoforms in the resistance to OS is novel and contrasts with the fact that most of p53 functions are attributed to the Δ Np53 (p53A) isoform in *Drosophila* [5]. Indeed, Δ Np53 (p53A) is the main isoform expressed in developing and normal fly tissues and is responsible for the induction of apoptosis in response to irradiation (FlyBase FBgn0039044 and [18]). In contrast, p53 (p53B) expression is mainly restricted to reproductive organs where it is required for programmed necrosis during spermatogenesis [3]. Thus, depending on tissue type and stress, a single or both isoforms are required to induce an appropriate p53 biological response. Our results also suggest that p53 is required for protection against OS by maintaining functional levels of basal

autophagy in *Drosophila*. Indeed, $p53^{null}$ mutant flies exhibit a decreased resistance to PQ that is associated with an impaired autophagic flux. The defective autophagy could be a direct consequence of reduced autophagy activation in flies lacking $p53$. However, we did not observe a $p53$ -dependent activation of autophagy after PQ treatment. In contrast, the basal autophagy was reduced in $p53^{null}$ mutant flies treated with PQ, indicating that $p53$ is not activating autophagy but rather that basal autophagy is impaired in the absence of $p53$. Thus, the defective autophagy is not due to a decrease of autophagy induction but could reflect a caspase-dependent inhibition of autophagic flux in $p53^{null}$ mutant exposed to PQ. To reconcile that $p53$ is protective in flies treated with PQ with the fact that overexpression of $\Delta Np53$ ($p53A$) or $p53$ ($p53B$) induces cell death when overexpressed in PRs, we propose that $p53$ responses and the outcome survival or death depends on $p53$ levels of expression (Figure 7). In PQ-treated flies, $p53$ is induced at physiological level, and is required for cell and organismal survival possibly by promoting an anti-oxidant response as previously proposed [54,55]. In contrast, overexpression of $\Delta Np53$ ($p53A$) or $p53$ ($p53B$), under the strong *ninaE/Rh1* driver, activates autophagy and caspase-dependent or caspase-independent cell death, respectively, ultimately leading to cell demise. These results reveal distinct $p53$ responses, with the outcome – survival or death – depending not only on the intensity and duration of stress as previously proposed [56,57] but also on the levels of each $p53$ isoform. In conclusion, our data bring novel insights to the model on the flexibility of the pleiotropic $p53$ gene in inducing a single context-appropriate pathway to protect the organism [5].

Materials and methods

Fly strains and genetic manipulations

Flies were reared at 25°C in a 12 h/12 h light-dark cycle. The following lines were used: w^{1118} (WT), $p53^{5A-1-4}$ null allele [58] (Bloomington Stock center, BL6815), *atg8a*^{KG07569} null allele (Bloomington stock center, BL14639 [59]), and *drone*¹²⁹ (gift of Dr. A. Bergman). In overexpression experiments, *ninaE/rh1-gal4* line (gift of J. Treisman [60]) or the *da-gal4* line (Bloomington stock center) were crossed with *UAS-GFP-ref(2)P* (gift of T. Neufeld [61]), *UAS-GFP-LC3* (*UAS-GFP-Atg8a*) gift of H. Stenmark (Department of Molecular Cell Biology, Institute for Cancer Research, Oslo, Norway) [62]), *UAS-mCherry-GFP-Atg8a* (gift of I. Nezis (School of Life Sciences, University of Warwick, Coventry, United Kingdom) [43]), *UAS-mCD8-RFP*, *UAS-LacZ* (Bloomington Stock center), *UAS-p53*, *UAS-ΔNp53* [17], *UAS-p35* (Bloomington stock center), *UAS-luciferase IR* (Bloomington stock center), *UAS-dcp-1 IR* (VDRC34328), *UAS-drice IR* (VDRC28064), *UAS-p53 IR* (VDRC10692), or *UAS-p53 IR* (VDRC45138). The *ey-flp*, *ninaE/rh1-GAL4;UAS-GFP;FRT80 UAS-tdTomato* line was described previously [44,45] and was crossed with the *ninaE/rh1-gal4* line to generate clones with *atg1Δ3D FRT80* stocks (gift from T. Neufeld (Department of Genetics, University of Minnesota, Minneapolis, USA) [63]). *Cherry-p53B STOP*; $p53^{5A-1-4}$

(FlyBase FBal0318401) (here named Ch- $p53B STOP$) and *GFP-p53A STOP*; $p53^{5A-1-4}$ (FlyBase FBal0318403) (here named GFP- $p53A STOP$) were previously reported [18].

Transformation with $p53BAC$ and generations of $\Delta Np53$ ($p53A$) alleles by CRISPR-Cas9

$p53BAC$ flies carrying a wild-type $p53$ genomic BAC clone of 21-kilobase in the P[acman] system [64] were injected to generate transgenic lines using $\Phi C31$ integrase-mediated transgenesis (Best Gene, Inc. Chino Hills, CA, USA). Vector DNA was injected in embryos carrying attP docking sites on the second chromosome (strain 9736 at 53B2).

The $\Delta Np53$ ($p53A$) isoform-specific alleles were made using CRISPR-Cas9 methods as described [65]. The $p53^{A2.3}$ allele is a 23 bp deletion that spans the first $\Delta Np53$ ($p53A$) transcript exon/intron junction (coordinates 23053346--23053368 in the *D. melanogaster* genome version 6), with a 7 base-pair insertion of TACTGCT. This allele deletes part of the unique $\Delta Np53$ ($p53A$) coding sequence and the splice donor site. The $p53^{A39.4}$ allele is a 29 base pair deletion (coordinates 23053338–23053366), which also spans the first $\Delta Np53$ ($p53A$) exon/intron junction, deleting part of the first unique exon that encodes $\Delta Np53$ ($p53A$) and the RNA splice donor site.

Chemical treatments

Paraquat (Sigma, 36541) was freshly added to phosphate-buffered saline (PBS Dubelccos; Invitrogen Life Technologies, 14200067) containing 0.8% low melting agarose (Sigma, A9414) and 10% sucrose (Sigma, S0389) shortly before the experiment. Twenty flies (3 d of age) were fed with 20 mM paraquat (Sigma, 36541)-containing medium for 5–7 d (survival experiments) or 21 h (protein or RNA extractions and brain dissections). Unless otherwise indicated, flies were kept at 25°C throughout the experiment.

Live fluorescence imaging of PRs

CO₂-anesthetized flies were placed in a 35-mm cell culture dish half-filled with 1% agarose, covered with water at 4°C, and observed using a confocal microscope (LSM700; Carl Zeiss Microscopy GmbH, Göttingen, Germany) as described previously [44,66].

Retina dissection and immunostaining

Retinas of 3-day-old flies were dissected following the standard procedure described in [67]. Briefly, heads were kept in a drop of PBS to avoid drying. One eye was then cut off using a scalpel and the cuticle around the eye removed. Finally, the brain parts attached to the retina were carefully removed using forceps. Samples were conserved in 4% paraformaldehyde (PFA)-PBS on ice until all the retinas had been dissected, and they were then fixed for 20 min at room temperature (RT). After fixing, the samples were washed 3 times in 0.3% Triton X-100 (Sigma, T8787) in PBS (0.3% PBS-T) and incubated with polyclonal rabbit anti-GFP (Invitrogen, A6455;

1:200) or monoclonal rabbit anti-cleaved Dcp-1 (Cell Signaling Technology, 9578S; 1:300) in 0.1% Triton X-100, 4% normal goat serum (Sigma, G9023), PBS for 16 h at 4°C. The samples were washed 3 times in washing solution and incubated with anti-rabbit Alexa Fluor 488 (Invitrogen, A21206; 1:500) or anti-rabbit Alexa Fluor 546 (Invitrogen, A10040; 1:500) secondary antibody, as appropriate. Samples were also incubated with phalloidin-rhodamine (Sigma, 77,418; 1:400) or phalloidin-633 (Sigma, 68,825; 1:400) to better visualize the PR cells. Finally, samples were washed 3 times and embedded in Vectashield medium containing DAPI (Vectashield, AbCys, H1200), mounted, and stored at 4°C until visualization. For the analysis of the mCherry-GFP-Atg8a signal, samples were washed in 0.1% PBS-T after fixation and immediately mounted for visualization.

Brain dissection and immunostaining

Brains of paraquat (PQ)- or control-treated flies were dissected at RT in Ringer solution (Sigma, 96724) and fixed for 2 h on ice in 4% PFA in PBS. After 3 15-min washes in 0.5% PBS-T, tissues were blocked for 2 h in 2% bovine serum albumin fraction V (Sigma, A2153) in 0.5% PBS-T. Brains were incubated overnight at 4°C in blocking solution containing rabbit anti-cleaved human CASP3/caspase 3 (Asp175) mAb (1:100; Cell Signaling Technology, 9661). After 3 15-min washes in 0.5% PBS-T, brains were incubated for 2 h at RT with Alexa Fluor 488 anti-rabbit (1:1000; Invitrogen, A21206). Tissues were washed 3 times in 0.5% PBS-T for 15 min and then mounted in ProLong Gold Antifade Mountant (Life Technologies, P36930).

Transmission electron microscopy

Dissected *Drosophila* eyes were fixed in 0.1 M cacodylate buffer, 2.5% glutaraldehyde, and 2 mM CaCl₂ for 16 h at 4°C. After rinsing with 0.1 M cacodylate buffer at RT, the eyes were incubated with 1% OsO₄ in 0.1 M cacodylate buffer for 2 h at RT. Tissues were then progressively dehydrated in acetone at RT and mounted in 100% epoxy resin (Epon 812; Electronic Microscopy Sciences, 14120) in silicone-embedding molds. After resin polymerization for 48 h at 60°C, samples were sliced into 60-nm sections, which were stained with lead citrate and examined with a Philips CM120 (Thermo Fischer Scientific, Eindhoven, The Netherlands) transmission electron microscope (TEM) operating at 80 kV.

Image processing

Images were acquired at the imaging facility (PLATIM, UMS3444) at the UMR8249 imaging facility and analyzed with ImageJ (National Institutes of Health) or with Fiji software. For retina immunostaining, images were acquired on acousto-optical beam splitter confocal laser-scanning microscopes (SP5; Leica Microsystems, Wetzlar, Germany) with an HCX Plan Achromat 63 × 1.4–0.6 oil (numerical aperture: 1.4) objective using the acquisition software LAS AF (Leica). For whole-mount brain staining, images were acquired on an A1R confocal microscope (Nikon Instrument, Tokyo, Japan) with a 40× objective using NIS-Elements Advanced Research

software (Nikon). For live imaging of PRs, images were acquired on a confocal laser-scanning microscope (LSM700; Carl Zeiss Microscopy GmbH, Göttingen, Germany) with an immersion 40 × 0.75 water (numerical aperture: 0.75) objective using the acquisition software Zen (Zeiss).

Protein extracts and western blotting analysis

Proteins were extracted from 3 or 4 whole animals after treatment (4-day-old flies) using a standard protocol. Briefly, anesthetized or frozen flies were squashed in extraction buffer (1% NP40; abcam ab142227), 20 mM Tris HCl, pH 7.5, 100 mM NaCl, 2 mM DTT, and protease inhibitor cocktail (Roche, 11836153001), incubated on ice for 30 min, and centrifuged for 30 min at 12,000 g. An aliquot (1 µl) of the supernatant was then tested in a Bradford protein assay reaction (Bio-Rad, 500–0201). The samples were boiled, and 50 µg of protein per lane were resolved by SDS-PAGE using 15% gels for the analysis of endogenous Atg8 and cleaved Dcp-1 and 4–20% gels (Bio-Rad, 456–1093) for detection of ref(2)P, endogenous Atg8, and cleaved Dcp-1 simultaneously. After electrophoresis, proteins were transferred to PVDF (for endogenous Atg8) or nitrocellulose membranes, blocked for 1 h in TBS (50 mM Tris-HCl pH 7, 0.15 M NaCl in ddH₂O) containing 0.1% Tween 20 (Sigma, P7949) (0.1% TBS-T) and 5% milk and then incubated at 4°C for 16 h in 0.1% TBS-Tween, 1% milk containing rabbit anti-cleaved Dcp-1 (1:1000; Cell Signaling Technology, 9578S), rabbit anti-cleaved human CASP3 (Asp175) (1:1000; Cell Signaling Technology, 9661), mouse anti-TUBA/α-tubulin (1:1000; Sigma, T6199), anti-Atg8 (1:5,000; gift of G. Juhasz (Department of Anatomy, University of Budapest, Hungary) [68], or rabbit anti-ref(2)P (1:500; gift of S. Gaumer (Laboratoire de Génétique et de Biologie Cellulaire, Université de Saint-Quentin-en-Yvelines, Montigny le Bretonneux, France) [34]. Membranes were washed 3 times in 0.1% TBS-T for 10 min and incubated at RT for 2 h in 0.1% TBS-T/1% milk containing anti-rabbit HRP (1:10,000; GE Healthcare, NA9340) or anti-mouse HRP (1:10,000; GE Healthcare, NA9310) secondary antibody, as appropriate. After 3 washes, proteins were revealed using ECL prime (GE Healthcare, RPN2232) according to the kit protocol. Western blot analysis of the *p53* CRISPR alleles was performed with anti-human TP/p53 (Santa Cruz Biotechnology, C11) on protein extracts from adult flies 4 h after irradiation with 4000 rads of gamma rays as described previously [18,69].

RT-PCR

Expression of *p53* (*p53B*) and $\Delta Np53$ (*p53A*) were monitored by RT-PCR. RNA was extracted from adult flies using TRIzol reagent (Invitrogen, 15596026) and cDNA was produced using the SuperScript III First Strand Synthesis System (Invitrogen, 18080044) with random hexamers.

PCR was performed using the following primers: *p53* (*p53B*) forward: GGACACAAATCGCAACTGCT, $\Delta Np53$ (*p53A*) forward: CACAGCCAATGTCGTGGCAC, and a common reverse primer for *p53* (*p53B*) and $\Delta Np53$ (*p53A*): GGCCATGGGTTCCGTGGTCA. Amplicons of $\Delta Np53$ (*p53A*) (129 base pairs [bp]) and *p53* (*p53B*) (519 bp) were visualized after 30 and 35 cycles, respectively, with a melting

temperature of 60°C. Samples were resolved on a 2% agarose gel. *RpL32/rp49* was used as an internal control for RNA extraction and RT-PCR efficiency and was amplified using forward: ATCGTGAAGAAGCGCACCAAG and reverse: ACCAGGAACCTTCTTGAATCCG primers. Amplicons of *RpL32/rp49* (203 bp) were visualized after 25 cycles with a melting temperature of 60°C.

Image and statistical analyses

All microscopy and western blot images were analyzed using ImageJ software, with the exception of the western blot shown in Figure S1C, which was analyzed using Fiji. Quantification of GFP-ref(2)P and GFP-Atg8a was performed using the Find Maxima function of ImageJ. Western blots were quantified densitometrically.

Statistical analyses were performed using Prism software (GraphPad). In all figures, bar graphs represent the mean ± SEM. For survival experiments, the results were analyzed using two-way ANOVA with the Tukey multiple comparison post hoc test. Quantification of western blots and caspase staining in the brain was analyzed using one-way ANOVA and the Bonferroni post hoc test. For all other experiments, the results were analyzed using the Student t test.

List of abbreviations

Atg1	autophagy-related 1
Atg8a/LC3	autophagy-related 8a
Ch-p53B	Cherry-p53B
Dcp-1	Death caspase-1
DNA	deoxyribonucleic acid
Drice	Death related ICE-like caspase
Dronc	Death regulator Nedd2-like caspase
ECL	enhanced chemiluminescence
ey	eyeless
flp	flipper
GFP	green fluorescent protein
GMR	glass multiple reporter
HRP	horseradish peroxidase
LacZ	β-galactosidase
mCD8	membrane tagged cluster of differentiation
mCherry	monomeric Cherry
ninaE/Rh1	neither inactivation nor after potential E
PQ	paraquat
PR	photoreceptor; ref(2)P: refractory to sigma P
RNAi	ribonucleic acid interference
rpr	reaper
ROS	reactive oxygen species
SEM	standard error of the mean
TEM	transmission electron microscopy
UAS	upstream activating sequence
WT	wild-type.

Acknowledgments

We thank Dali Ma for for generating unpublished material related to this work, Michael Dixon for technical assistance, Daan Van Den Brink and Charlotte Scholtes for art work. We also thank A. Bergmann, J. Treisman, T. Neufeld, H. Stenmark, H.D. Ryoo, I. Nezis; the Bloomington, DGRC Kyoto, and VDRC stock centers; and DSHB for fly stocks and reagents. We thank the ARTHRO-TOOL fly, PLATIM (UMS3444 Biosciences Lyon) and the Centre

Technologique des Microstructures CTμ (Lyon 1) microscopy facilities. The authors declare no conflicts of interest.

Disclosure statement

No potential conflict of interest was reported by the authors.

Funding

This work was supported by ANR Ire1-PD (13-ISV4-0003-01) and ARC foundation, la Ligue contre le Cancer, Rhône, France 705 Parkinson, FINOVI (2017-01 26-A011) grants to BM, a Fondation de France (2012-00034435) grant to SB and BM, a Labex MemoLife (ANR-10-LABX-54 MEMO LIFE) grant to SB, and an NIH 1R01GM113107 to B.R.C. PMD was supported by FCT grants LISBOA-01-0145-FEDER- 007660, FCT-ANR/NEU-NMC/0006/2013, 710 PTDC/NEU-NMC/2459/2014, and IF/00697/2014.

ORCID

Ludivine Walter  <http://orcid.org/0000-0001-7214-0676>

Serge Birman  <http://orcid.org/0000-0002-4278-454X>

Bertrand Mollereau  <http://orcid.org/0000-0003-4710-8185>

References

- [1] Vousden KH, Lane DP. p53 in health and disease. *Nat Rev Mol Cell Biol.* 2007 Apr;8(4):275–283. PubMed PMID: 17380161.
- [2] Brady CA, Attardi LD. p53 at a glance. *J Cell Sci.* 2010 Aug 1;123 (Pt 15):2527–2532. PubMed PMID: 20940128; eng.
- [3] Napolitano F, Gibert B, Yacobi-Sharon K, et al. p53-dependent programmed necrosis controls germ cell homeostasis during spermatogenesis. *PLoS Genet.* 2017 Sep;13(9):e1007024. PubMed PMID: 28945745; eng.
- [4] Hager KM, Gu W. Understanding the non-canonical pathways involved in p53-mediated tumor suppression. *Carcinogenesis.* 2014 Dec 31;35(4):740–746. PubMed PMID: 24381013; Eng. .
- [5] Mollereau B, Ma D. The p53 control of apoptosis and proliferation: lessons from *Drosophila*. *Apoptosis.* 2014 Oct;19 (10):1421–1429. PubMed PMID: 25217223; eng. .
- [6] He C, Klionsky DJ. Regulation mechanisms and signaling pathways of autophagy. *Annu Rev Genet.* 2009 Aug;4(43):67–93. PubMed PMID: 19653858.
- [7] Klionsky DJ, Abdelmohsen K, Abe A, et al. Guidelines for the use and interpretation of assays for monitoring autophagy (3rd edition). *Autophagy.* 2016;12(1):1–222. PubMed PMID: 26799652; PubMed Central PMCID: PMC4835977. eng.
- [8] Hetz C, Mollereau B. Disturbance of endoplasmic reticulum proteostasis in neurodegenerative diseases. *Nat Rev Neurosci.* 2014 Apr;15 (4):233–249. Epub 2014 Mar 12. PubMed PMID: 24619348; eng.
- [9] Marcel V, Dichtel-Danjoy M-L, Sagne C, et al. Biological functions of p53 isoforms through evolution: lessons from animal and cellular models. *Cell Death Differ.* 2011 Dec;18(12):1815–1824. Epub 2011 Sep 23. PubMed PMID: 21941372; eng.
- [10] Khoury MP, Bourdon JC. The Isoforms of the p53 Protein. *Cold Spring Harb Perspect Biol.* 2010 Mar;2(3):a000927. PubMed PMID: 20300206.
- [11] Bourdon JC. p53 Family isoforms. *Curr Pharm Biotechnol.* 2007 Dec;8(6):332–336. PubMed PMID: 18289041.
- [12] Marygold SJ, Crosby MA, Goodman JL. Using FlyBase, a Database of *Drosophila* Genes and Genomes. *Methods Mol Biol.* 2016;1478:1–31. PubMed PMID: 27730573; PubMed Central PMCID: PMC45107610. eng.
- [13] Ollmann M, Young LM, Di Como CJ, et al. *Drosophila* p53 is a structural and functional homolog of the tumor suppressor p53. *Cell.* 2000 Mar 31;101(1):91–101. PubMed PMID: 10778859.

- [14] Jin S, Martinek S, Joo WS, et al. Identification and characterization of a p53 homologue in *Drosophila melanogaster*. *Proc Natl Acad Sci U S A*. 2000;97(13):7301–7306. PubMed PMID: 10860994.
- [15] Brodsky MH, Nordstrom W, Tsang G, et al. *Drosophila* p53 binds a damage response element at the reaper locus. *Cell*. 2000;101(1):103–113. PubMed PMID: 10778860.
- [16] Bourdon J-C, Fernandes K, Murray-Zmijewski F, et al. p53 isoforms can regulate p53 transcriptional activity. *Genes Dev*. 2005 Sep 15;19(18):2122–2137. PubMed PMID: 16131611.
- [17] Dichtel-Danjoy M-L, Ma D, Dourlen P, et al. *Drosophila* p53 isoforms differentially regulate apoptosis and apoptosis-induced proliferation. *Cell Death Differ*. 2013 Jan;20(1):108–116. Epub 2012 Aug 17. PubMed PMID: 22898807; eng.
- [18] Zhang B, Rotelli M, Dixon M, et al. The function of *Drosophila* p53 isoforms in apoptosis. *Cell Death Differ*. 2015 Dec;22(12):2058–2067. PubMed PMID: 25882045; Eng.
- [19] Crighton D, Wilkinson S, Ryan KM. DRAM links autophagy to p53 and programmed cell death. *Autophagy*. 2007 Jan–Feb;3(1):72–74. PubMed PMID: 17102582; eng.
- [20] Crighton D, Wilkinson S, O'Prey J, et al. DRAM, a p53-induced modulator of autophagy, is critical for apoptosis. *Cell*. 2006 Jul 14;126(1):121–134. PubMed PMID: 16839881; eng.
- [21] Mollereau B. Cell death: what can we learn from flies? Editorial for the special review issue on *Drosophila* apoptosis. *Apoptosis*. 2009 Aug;14(8):929–934. PubMed PMID: 19629695.
- [22] Fan Y, Lee TV, Xu D, et al. Dual roles of *Drosophila* p53 in cell death and cell differentiation. *Cell Death Differ*. 2010 Jun;17(6):912–921. PubMed PMID: 19960025; PubMed Central PMCID: PMC3014827. eng. .
- [23] Mesquita D, Dekanty A, Milan M. A dp53-dependent mechanism involved in coordinating tissue growth in *Drosophila*. *PLoS Biol*. 2010;8(12):e1000566. PubMed PMID: 21179433; eng.
- [24] Lu W-J, Chapo J, Roig I, et al. Meiotic recombination provokes functional activation of the p53 regulatory network. *Science*. 2010 Jun 4;328(5983):1278–1281. PubMed PMID: 20522776.
- [25] de la Cova C, Senoo-Matsuda N, Ziosi M, et al. Supercompetitor status of *drosophila myc* cells requires p53 as a fitness sensor to reprogram metabolism and promote viability. *Cell Metab*. 2014 Mar 4;19(3):470–483. Epub 2014 Feb 20. PubMed PMID: 24561262; eng. .
- [26] Nakamura M, Ohsawa S, Igaki T. Mitochondrial defects trigger proliferation of neighbouring cells via a senescence-associated secretory phenotype in *Drosophila*. *Nat Commun*. 2014;5:5264. PubMed PMID: 25345385; eng.
- [27] Merlo P, Frost B, Peng S, et al. p53 prevents neurodegeneration by regulating synaptic genes. *Proc Natl Acad Sci U S A*. 2014 Dec 16;111(50):18055–18060. PubMed PMID: 25453105; Eng.
- [28] Arking R, Buck S, Berrios A, et al. Elevated paraquat resistance can be used as a bioassay for longevity in a genetically based long-lived strain of *Drosophila*. *Dev Genet*. 1991;12(5):362–370. PubMed PMID: 1806332; eng.
- [29] Wang MC, Bohmann D, Jasper H. JNK signaling confers tolerance to oxidative stress and extends lifespan in *Drosophila*. *Dev Cell*. 2003 Nov;5(5):811–816. PubMed PMID: 14602080.
- [30] Girardot F, Monnier V, Tricoire H. Genome wide analysis of common and specific stress responses in adult *drosophila melanogaster*. *BMC Genomics*. 2004 Sep 30;5(1):74. PubMed PMID: 15458575.
- [31] Juhasz G, Erdi B, Sass M, et al. Atg7-dependent autophagy promotes neuronal health, stress tolerance, and longevity but is dispensable for metamorphosis in *Drosophila*. *Genes Dev*. 2007 Dec 1;21(23):3061–3066. PubMed PMID: 18056421; eng.
- [32] Simonsen A, Cumming RC, Brech A, et al. Promoting basal levels of autophagy in the nervous system enhances longevity and oxidant resistance in adult *Drosophila*. *Autophagy*. 2008 Feb;4(2):176–184. PubMed PMID: 18059160; eng.
- [33] Crighton D, Wilkinson S, Ryan KM. DRAM links autophagy to p53 and programmed cell death. *Autophagy*. 2006 Jan–Feb;3(1):72–74. PubMed PMID: 17102582; eng.
- [34] Nezis IP, Simonsen A, Sagona AP, et al. Ref(2)P, the *Drosophila melanogaster* homologue of mammalian p62, is required for the formation of protein aggregates in adult brain. *J Cell Biol*. 2008 Mar 24;180(6):1065–1071. PubMed PMID: 18347073.
- [35] Cassar M, Issa A-R, Riemensperger T, et al. A dopamine receptor contributes to paraquat-induced neurotoxicity in *Drosophila*. *Hum Mol Genet*. 2015 Jan 1;24(1):197–212. PubMed PMID: 25158689; PubMed Central PMCID: PMC4326327. eng.
- [36] Querenet M, Goubard V, Chatelain G, et al. Spen is required for pigment cell survival during pupal development in *Drosophila*. *Dev Biol*. 2015 Jun 15;402(2):208–215. PubMed PMID: 25872184; Eng.
- [37] Fan Y, Bergmann A. The cleaved-Caspase-3 antibody is a marker of Caspase-9-like DRONC activity in *Drosophila*. *Cell Death Differ*. 2010 Mar;17(3):534–539. PubMed PMID: 19960024.
- [38] Mollereau B, Domingos PM. Photoreceptor differentiation in *Drosophila*: from immature neurons to functional photoreceptors. *Dev Dyn*. 2005 Mar;232(3):585–592. PubMed PMID: 15704118.
- [39] Mendes CS, Levet C, Chatelain G, et al. ER stress protects from retinal degeneration. *Embo J*. 2009 May 6;28(9):1296–1307. PubMed PMID: 19339992.
- [40] Nisoli I, Chauvin JP, Napoletano F, et al. Neurodegeneration by polyglutamine Atrophin is not rescued by induction of autophagy. *Cell Death Differ*. 2010 Mar 26;17(10):1577–1587. PubMed PMID: 20339376.
- [41] Jain A, Rusten TE, Katheder N, et al. p62/Sequestosome-1, Autophagy-related Gene 8, and Autophagy in *Drosophila* Are Regulated by Nuclear Factor Erythroid 2-related Factor 2 (NRF2), Independent of Transcription Factor TFEB. *J Biol Chem*. 2015 Jun 12;290(24):14945–14962. PubMed PMID: 25931115; PubMed Central PMCID: PMC4463441. eng.
- [42] Nagy P, Varga A, Kovacs AL, et al. How and why to study autophagy in *Drosophila*: it's more than just a garbage chute. *Methods*. 2015 Mar;75:151–161. PubMed PMID: 25481477; PubMed Central PMCID: PMC4358840. Eng.
- [43] Nezis IP, Shrivage BV, Sagona AP, et al. Autophagy as a trigger for cell death: autophagic degradation of inhibitor of apoptosis dBruce controls DNA fragmentation during late oogenesis in *Drosophila*. *Autophagy*. 2010 Nov;6(8):1214–1215. PubMed PMID: 20935512; eng.
- [44] Gambis A, Dourlen P, Steller H, et al. Two-color in vivo imaging of photoreceptor apoptosis and development in *Drosophila*. *Dev Biol*. 2011 Mar 1;351(1):128–134. PubMed PMID: 21215264.
- [45] Dourlen P, Bertin B, Chatelain G, et al. *Drosophila* fatty acid transport protein regulates rhodopsin-1 metabolism and is required for photoreceptor neuron survival. *PLoS Genet*. 2012 Jul;8(7):e1002833. PubMed PMID: 22844251; eng.
- [46] Ravikumar B, Berger Z, Vacher C, et al. Rapamycin pre-treatment protects against apoptosis. *Hum Mol Genet*. 2006 Apr 1;15(7):1209–1216. PubMed PMID: 16497721.
- [47] Yang D-S, Kumar A, Stavrides P, et al. Neuronal apoptosis and autophagy cross talk in aging PS/APP mice, a model of Alzheimer's disease. *Am J Pathol*. 2008 Sep;173(3):665–681. PubMed PMID: 18688038; eng.
- [48] Fouillet A, Levet C, Virgone A, et al. ER stress inhibits neuronal death by promoting autophagy. *Autophagy*. 2012 Jun;8(6):915–926. Epub 2012 Jun 1. PubMed PMID: 22660271; eng.
- [49] Nandi N, Tyra LK, Stenesen D, et al. Acinus integrates AKT1 and subapoptotic caspase activities to regulate basal autophagy. *J Cell Biol*. 2014 Oct 27;207(2):253–268. Epub 2014 Oct 20. PubMed PMID: 25332163; eng.
- [50] DeVorkin L, Go NE, Hou YC, et al. The *Drosophila* effector caspase Dcp-1 regulates mitochondrial dynamics and autophagic flux via SesB. *J Cell Biol*. 2014 May 26;205(4):477–492. PubMed PMID: 24862573; Eng.
- [51] Hou YC, Chittaranjan S, Barbosa SG, et al. Effector caspase Dcp-1 and IAP protein Bruce regulate starvation-induced autophagy during *Drosophila melanogaster* oogenesis. *J Cell Biol*. 2008 Sep 22;182(6):1127–1139. PubMed PMID: 18794330.

- [52] Benosman S, Meng X, Von Grabowiecki Y, et al. Complex regulation of p73 isoforms after alteration of amyloid precursor polypeptide (APP) function and DNA damage in neurons. *J Biol Chem.* 2011 Dec 16;286(50):43013–43025. PubMed PMID: 22002055; PubMed Central PMCID: PMC3234838. eng.
- [53] Turnquist C, Horikawa I, Foran E, et al. p53 isoforms regulate astrocyte-mediated neuroprotection and neurodegeneration. *Cell Death Differ.* 2016 Sep 1;23(9):1515–1528. PubMed PMID: 27104929; PubMed Central PMCID: PMC5072428. eng.
- [54] Sablina AA, Budanov AV, Ilyinskaya GV, et al. The antioxidant function of the p53 tumor suppressor. *Nat Med.* 2005 Dec;11(12):1306–1313. PubMed PMID: 16286925.
- [55] Nam SY, Sabapathy K. p53 promotes cellular survival in a context-dependent manner by directly inducing the expression of haeme-oxygenase-1. *Oncogene.* 2011 Nov 3;30(44):4476–4486. PubMed PMID: 21552291; eng.
- [56] Oren M. Decision making by p53: life, death and cancer. *Cell Death Differ.* 2003 Apr;10(4):431–442. PubMed PMID: 12719720.
- [57] Horn HF, Vousden KH. Coping with stress: multiple ways to activate p53. *Oncogene.* 2007 Feb 26;26(9):1306–1316. PubMed PMID: 17322916.
- [58] Rong YS, Titen SW, Xie HB, et al. Targeted mutagenesis by homologous recombination in *D. melanogaster*. *Genes Dev.* 2002 Jun 15;16(12):1568–1581. PubMed PMID: 12080094.
- [59] Scott RC, Juhasz G, Neufeld TP. Direct induction of autophagy by atg1 inhibits cell growth and induces apoptotic cell death. *Curr Biol.* 2007 Jan 9;17(1):1–11. PubMed PMID: 17208179.
- [60] Mollereau B, Wernet MF, Beaufils P, et al. A green fluorescent protein enhancer trap screen in *Drosophila* photoreceptor cells. *Mech Dev.* 2000;93(1–2):151–160.
- [61] Chang YY, Neufeld TP. An Atg1/Atg13 complex with multiple roles in TOR-mediated autophagy regulation. *Mol Biol Cell.* 2009 Apr;20(7):2004–2014. PubMed PMID: 19225150.
- [62] Rusten TE, Lindmo K, Juhasz G, et al. Programmed autophagy in the *Drosophila* fat body is induced by ecdysone through regulation of the PI3K pathway. *Dev Cell.* 2004 Aug;7(2):179–192. PubMed PMID: 15296715.
- [63] Scott RC, Schuldiner O, Neufeld TP. Role and regulation of starvation-induced autophagy in the *Drosophila* fat body. *Dev Cell.* 2004 Aug;7(2):167–178. PubMed PMID: 15296714.
- [64] Venken KJ, Carlson JW, Schulze KL, et al. Versatile P[acman] BAC libraries for transgenesis studies in *Drosophila melanogaster*. *Nat Methods.* 2009 6;Jun(6):431–434. PubMed PMID: 19465919.
- [65] Gratz SJ, Cummings AM, Nguyen JN, et al. Genome engineering of *Drosophila* with the CRISPR RNA-guided Cas9 nuclease. *Genetics.* 2013 Aug;194(4):1029–1035. PubMed PMID: 23709638; PubMed Central PMCID: PMC3730909. eng.
- [66] Dourlen P, Levet C, Mejat A, et al. The Tomato/GFP-FLP/FRT method for live imaging of mosaic adult *drosophila* photoreceptor cells. *J Vis Exp.* 2013;(79). DOI:10.3791/50610. PubMed PMID: 24084155; Eng.
- [67] Domingos PM, Brown S, Barrio R, et al. Regulation of R7 and R8 differentiation by the spalt genes. *Dev Biol.* 2004 Sep 1;273(1):121–133. PubMed PMID: 15302602.
- [68] Nagy P, Karpati M, Varga A, et al. Atg17/FIP200 localizes to perilyosomal Ref(2)P aggregates and promotes autophagy by activation of Atg1 in *Drosophila*. *Autophagy.* 2014 Mar;10(3):453–467. Epub 2014 Jan 6. PubMed PMID: 24419107; eng.
- [69] Zhang B, Mehrotra S, Ng WL, et al. Low levels of p53 protein and chromatin silencing of p53 target genes repress apoptosis in *drosophila* endocycling cells. *PLoS Genet.* 2014 Sep;10(9):e1004581. eCollection 2014 Sep. PubMed PMID: 25211335; eng.